Proc. Natl. Acad. Sci. USA
Vol. 94, pp. 2951–2956, April 1997
Biochemistry

Single-strand DNA intermediates in phage λ's Red recombination pathway

STUART A. HILL*†, MARY M. STAHL*‡, AND FRANKLIN W. STAHL*§

*Institute of Molecular Biology, University of Oregon, Eugene, OR 97403-1229; and †Laboratory of Microbial Structure and Function, National Institutes of Health, National Institute of Allergy and Infectious Disease, Rocky Mountain Laboratories, Hamilton, MT 59840-2999

Contributed by Franklin W. Stahl, January 22, 1997

ABSTRACT **An assay was developed to assess early intermediates arising in λ's Red recombination pathway. Double-strand breaks were delivered *in vivo* to nonreplicating λ chromosomes. Analysis by blot hybridization of total DNA extracts revealed the following: (*i*) long (>1.4 kilobases) single-strand DNA (ssDNA) intermediates; (*ii*) resection proceeding bidirectionally from the break site; (*iii*) single-strand overhangs of 3′ polarity; and (*iv*) in the absence of λ's *ninR* functions, a requirement of the *redα* gene product for the production of ssDNA. Therefore, the physical characteristics exhibited by these ssDNA molecules are consistent with their being an early recombination intermediate in the Red recombination pathway as proposed previously from genetic and *in vitro* biochemical analyses.**

When phage λ infects *Escherichia coli*, the principal recombination pathway (RecBCD) of the host is inactivated by the action of λ's *gam* gene product (Redγ). Phage recombination is then effected by the λ-encoded Red recombination pathway. When DNA replication is blocked, recombination is focused toward the ends of λ's linkage map (1). The localization of recombination events at the ends of the map reflects the presence of DNA ends arising from *cos*-cutting by the λ enzyme terminase, which cleaves the chromosome in readiness for packaging (2).

Analysis of recombinants produced under replication-blocked conditions *in vivo* has provided evidence for heteroduplex DNA splices (3–5). The strand polarity of these splices suggested the existence of an intermediate with a single-strand 3′ overhang, which could result from the action of λ's *redα* gene product (λ Red exonuclease). The *redα* gene product is a 5′-to-3′ double-strand-specific exonuclease; the *redβ* gene product is a DNA-melting protein (6–8). In cells lacking RecA protein, mutation in either *redα* or *redβ* eliminates recombination. In $RecA^+$ cells the recombination defect is less severe, presumably because of the activity of secondary bacterial recombination pathways.

Genetic studies of λ's Red pathway have demonstrated that recombination is initiated not only at *cos* but also at other duplex ends (9). When breaks were introduced into λ's chromosome through cleavage with a type II restriction endonuclease acting *in vivo*, recombination was stimulated and was focused around the incision. These observations were fortified by physical analyses of recombinant progeny phage particles (2). Similar observations have been made with the budding yeast *Saccharomyces cerevisiae*, where mating-type switches and meiotic recombination can be initiated by a double-strand break (DSB) in one of two interacting homologous chromosomes or regions (10–14).

The models proposed for λ's Red pathway operating under $RecA^+$ conditions (Fig. 1) and for events during meiotic recombination in yeast (15) are remarkably similar. A central feature of both models is that recombination involves invasion of an intact chromosome by a 3′ single-stranded region created at the site of the DSB. In yeast, meiotic recombination intermediates with 3′ single-stranded regions were identified at recombination hotspots (10, 11, 14, 16). Intermediates arose at a sufficiently well-defined time and were sufficiently stable (hours) (10, 17) to be amenable to characterization (14).

In this study, we demonstrate an early recombination intermediate that arises *in vivo* following the delivery of a defined DSB to a λ chromosome in the presence of the Red recombination pathway.

MATERIALS AND METHODS

Bacterial Strains and λ Genetic Elements. Crosses were performed in *Escherichia coli* strains FA77 (*dnaB*ts Su^-) (18), FWS2520 (*dnaB*ts *recJ*::Tn*10* Su^-) (our collection), and FWS3282 (*dnaB*ts D(*srlR-recA*) 306::Tn*10* Su^-) each containing pPAORM3.8 (19). All phage (Tables 1 and 2) were constructed by using standard *in vivo* techniques (27).

Preparation of Phage Stocks. The temperature-sensitive *c*I*857* allele, in conjunction with the *S7* mutation, allowed high-titer phage stocks to be prepared by heat induction. *Xho*I-modified phage stocks were prepared by inducing lysogens carrying the plasmid pPAORM3.8, which encodes the *Pae*R7 restriction–modification system (*Pae*R7 is an isoschizomer of *Xho*I) (19). Lysogenic cultures (50 ml) were grown at 34°C in LBK broth (1% tryptone/0.5% yeast extract/1% NaCl/75 mM $CaCl_2$/4 mM $FeCl_2$/2 mM $MgSO_4$/0.1 mg/ml vitamin B1) to a density of approximately 1×10^8 cells per ml. The culture was then incubated at 43°C for 15 min, followed by incubation with vigorous shaking at 37°C for 3 hr. Cells were harvested by centrifugation, and lysed in 2 ml of 10 mM Tris·HCl, pH 8.0/300 mM NaCl/5 mM sodium citrate by the combined action of lysozyme and chloroform. After lysis, 10 units of DNase I (molecular biology grade, United States Biochemical) were added, followed by incubation at 37°C for 30 min. Cell debris was removed by centrifugation, and the phage suspension was stabilized by the addition of $MgSO_4$ to a final concentration of 20 mM. Phage were further purified by banding in a CsCl equilibrium gradient, followed by dialysis against TM buffer (10 mM Tris·HCl, pH 8.0/10 mM $MgSO_4$). Phage were titered by plaque assay following serial dilution in TM buffer.

Cross Conditions. Host cells carrying the plasmid pPAORM3.8 were grown from an overnight culture at 26°C in cross broth (1% tryptone/0.5% NaCl supplemented with 0.2% maltose and 0.1 mg/ml vitamin B1 plus 100 μg/ml carbenicillin)

The publication costs of this article were defrayed in part by page charge payment. This article must therefore be hereby marked "*advertisement*" in accordance with 18 U.S.C. §1734 solely to indicate this fact.

0027-8424/97/942951-6$2.00/0
PNAS is available online at **http://www.pnas.org**.

Abbreviations: DSB, double-strand break; ssDNA, single-strand DNA.

‡Deceased January 22, 1996.
§To whom reprint requests should be addressed. e-mail: fstahl@molbio.uoregon.edu.

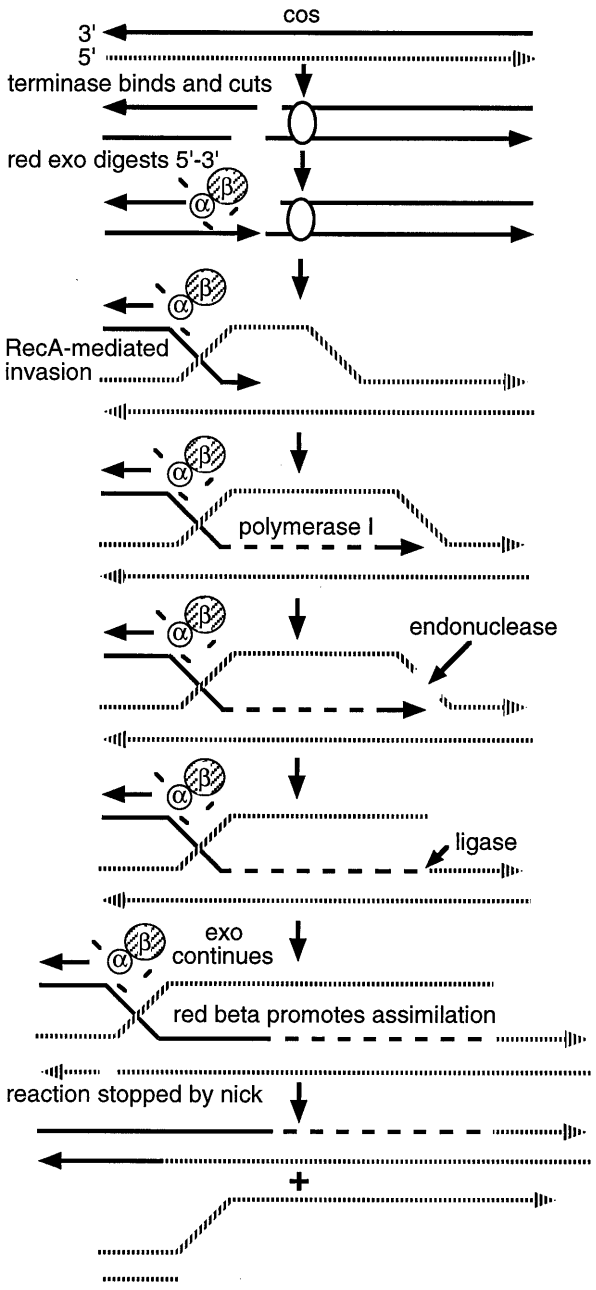

FIG. 1. The Red model for lytic cycle λ crosses conducted with blocked DNA replication in *rec*$^+$ cells (1). (*i*) λ's chromosome is cleaved at *cos* by the λ-encoded enzyme terminase; (*ii*) the cleaved chromosome is now a substrate for λ's *redα*/*β* gene products, resulting in single-strand overhangs of 3′ polarity; (*iii*) the single-strand overhang now invades a homologous uncut chromosome; (*iv*) DNA polymerase I extends the invasive strand; (*v*) a nick is introduced, possibly through endonucleolytic activity residing in DNA polymerase I; DNA ligase then ligates the invading strand with the nicked strand; and (*vi*) the Redβ protein completes assimilation of the invading strand until assimilation is stopped by encounter with an incidental nick.

to a density of ≈3 × 10^8 per ml. Ten-millliter aliquots were centrifuged at 4°C and cells were resuspended in 10 ml of prewarmed (43°C) TM buffer. Prewarmed *Xho*I-modified phage were added at a multiplicity of infection (moi) of 8, and the culture was supplemented with 10 ml of prewarmed 2× cross broth. After a 15-min incubation of the infected culture at 43°C (to express the *red* gene products), prewarmed unmodified phage were added at a moi of 8, and the infection was allowed to proceed for various lengths of time. Crosses were terminated by removing aliquots of cells and immediately placing them in an ethanol/water ice bath; cells were then concentrated by centrifugation at 4°C and stored at −20°C prior to DNA extraction. Infected cells blocked for λ DNA replication do not lyse spontaneously.

Table 1. Phage genotypes

Phage	Relevant genotype	Ref.
STU4	*cI857 P80 S7*	This study
MMS2560	*gam210 cI857 P80 S7*	This study
MMS2597	*gam210 cI857 P80 nin5 S7*	This study
MMS2408	*b1451 cI857 P80 S7*	This study
MMS2453	*red329 cI857 P80 S7*	This study
MMS2451	*b1451 cI857 P80 nin5 S7*	This study
MMS2649	*red113 cI857 P80 S7*	This study
MMS2484	*red113 cI857 P80 nin5 S7*	This study
MMS2650	*red15 cI857 P80 S7*	This study
MMS2485	*cI857 P80 nin5 S7*	This study
MMS2531	*XhoI*::*EcoRI cI857 P80 S7*	This study
MMS2444	*SR1*::*XhoI XhoI*::*EcoRI cI857 P80 S7*	This study

DNA Extraction. DNA extraction was performed as described by Ausubel *et al.* (28). Infected cells were resuspended in 2.5 ml of TE buffer (10 mM Tris·HCl, pH 8.0/1 mM EDTA) to which 25 μl of lysozyme at 5 mg/ml was added, followed by 5 min incubation at 37°C; 100 ml of 10% sodium dodecyl sulfate (SDS) and 5 μl of proteinase K (20 mg/ml) were then added, and incubation was continued at 37°C for 2 hr. A 300-μl aliquot of 5 M NaCl was added followed by gentle mixing and addition of 300 μl of 10% cetyltrimethylammonium bromide (CTAB; United States Biochemical) in 0.7 M NaCl. The lysate was shaken gently and incubated at 60°C for 10 min. The mixture was extracted with 2.5 ml of chloroform/isoamyl alcohol (20:1, vol/vol) and then centrifuged. The aqueous phase was further extracted with 2.5 ml of saturated phenol/chloroform. The DNA was precipitated with an equal volume of isopropyl alcohol, washed one time with 70% ethanol, and air dried. The DNA was then resuspended in 100 μl of TE buffer, pH 8.0.

DNA Analysis. Equivalent aliquots of total DNA were digested with restriction endonucleases, fractionated by agarose gel electrophoresis, and transferred through capillary action to nitrocellulose membranes either in the absence of prior denaturation [native conditions (29)] or after denaturation and neutralization (30). When DNA samples were treated with S1 nuclease, they were first digested with restriction endonuclease, precipitated with ethanol, and resuspended in nuclease buffer (10 mM Tris·HCl, pH 7.9/10 mM $MgCl_2$/200 mM NaCl/1 mM $ZnSO_4$/1 mM dithiothreitol). One unit of S1 nuclease (Boehringer Mannheim) was added followed by incubation at 30°C for 30 min. Blots were probed either with defined oligonucleotides that had been end-labeled with

Table 2. λ genetic elements

Element	Description and ref.
cI857	Temperature-sensitive allele of *c*I for heat induction of lysogens (20)
P80	Suppressor-sensitive (*sus*) allele of *P* that provides a partial replication block (21)
S7	*sus* allele of *S* suppressible only by SuIII (22)
b1451	Δ*redα* (23)
red329	*sus* mutation in *redα* (24)
red113	*sus* mutation in *redβ* (24)
gam210	*sus* mutation in *redγ* (25)
red15	Δ*redα*/*β* (23)
nin5	Δ*ninR* region (26)
SR1::*XhoI*	Insertion of an *XhoI* linker at position 21226 (*)
XhoI::*EcoRI*	Mutant *XhoI* site (*)

*F.W.S. and M.M.S., unpublished work.

[γ-^{32}P]ATP by using T4 polynucleotide kinase (New England Biolabs) or with various defined random primed DNA (either to the left or the right of the *Xho*I cut site) fragments labeled with [α-^{32}P]ATP by using a random prime labeling kit as specified by the manufacturer (Promega). The sequences of the oligonucleotides used were as follows:

probe 54 5′-TTGCAGGGTGGCCTGTTGCTGGCTG-3′;
probe 53 5′-CAGCCAGCAACAGGCCACCCTGCAA-3′;
probe 249 5′-GCGCCAGCATGATTAATACAGC-3′; and
probe 250 5′-GCTGTATTAATCATGCTGGCGC-3′.

The blots were visualized by autoradiography at −70°C using Kodak X-Omat film. Densitometric scanning of autoradiographs utilized an LKB 2222–020 UltroScan XL (Pharmacia Biotech, Piscataway, NJ).

RESULTS

Experimental Design. The following considerations influenced the experimental design: (*i*) in λ phage crosses blocked for DNA replication a DSB delivered by a restriction enzyme acting *in vivo* on an unmodified parent promoted recombination focused at the break site (2); and (*ii*) the identification of yeast meiotic recombination intermediates was possible using yeast cultures synchronized for meiosis (10, 11, 14, 16). Highly synchronous λ phage infections can be achieved by adsorbing phage to cells resuspended in TM buffer at 4°C, followed by a rapid elevation of temperature to 37°C (31). However, crosses conducted under these conditions do not allow for the maintenance of a tight replication block (achieved with a *P80* mutation in the phage chromosome and a *dnaB*ts host mutation). Consequently, we sacrificed tight synchrony for maintenance of the double replication block by adding the unmodified parent phage in TM buffer plus growth medium at 43°C. Measurements of unabsorbed phage showed that about 70% of the unmodified phage preparation infected the host cells within the first 15 min; the remainder continued to infect throughout the course of the experiment. Generally <1% remained in the culture supernatant at the end of the experiment (data not shown).

Identification of Single-Strand DNA (ssDNA) Recombination Intermediates. A defined break was introduced *in vivo* at λ's unique *Xho*I site by superinfecting strain FA77 (*rec*$^+$) carrying the *Pae*R7 restriction system on plasmid pPAORM3.8 (henceforth referred to as the *Xho*I system) with STU4 phage (wild type for λ's Red functions; from now on referred to as wild-type λ). Prior infection with modified phage allowed for the expression of λ's Red functions (9) and also provided intact homology. If early recombination events proceed as outlined in Fig. 2, then the following intermediates should be demonstrable: intermediate I, the *Xho*I double strand cut fragment (expected size following *in vitro Eco*RI digestion of total DNA extracts, 1751 bp); intermediate II, a ssDNA fragment where resection has not proceeded past the proximal *Eco*RI site (expected mobility approximately equivalent to 1751 bp); and intermediate III, an ssDNA fragment in which resection has proceeded past the proximal *Eco*RI site (expected mobility approximately equivalent to 7394 bp).

Samples were collected at various times after the addition of the unmodified (cuttable) phage. Total DNA extracts were prepared from each collected sample and digested *in vitro* with *Eco*RI (Fig. 3). Fragments were separated by gel electrophoresis and blotted under nondenaturing (29) or denaturing (30) conditions. After hybridization with appropriate probes (see *Materials and Methods* and Fig. 2), denatured blots (Fig. 3*A*) showed the following: (*i*) a signal that corresponded in mobility to the modified uncuttable helper phage (band a, 7421 bp; Fig. 3*A*); (*ii*) a signal that corresponded in mobility to the double-stranded DNA *Xho*I-cut fragment (band b, 1751 bp; Fig. 3*A*); and (*iii*) two other less intense signals (bands c and d; Fig. 3*A*) that migrated slightly faster than the signals designated a and b (Fig. 3*A*). The double-stranded DNA *Xho*I-cut fragment (band b; Fig. 3*A*) could be detected immediately after the addition of the unmodified phage stock (<30 sec) (data not shown).

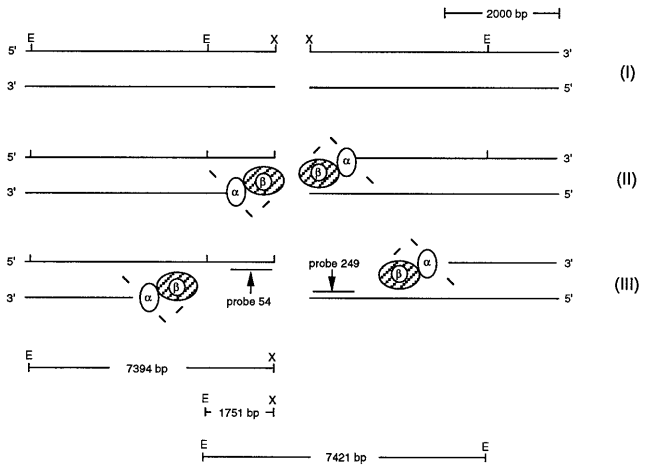

FIG. 2. Formation of ssDNAs after delivery of a double chain break at λ's *Xho*I site. A schematic representation of events following the delivery of a double chain break at λ's *Xho*I (X) site (intermediate I). After cleavage, the 5′ DNA end is resected using λ's Redα/β complex (intermediate II) exposing 3′ single-strand overhangs. Once the α/β complex passes the proximal *Eco*RI (E) site, this site becomes unavailable for restriction *in vitro*, leading to the formation of intermediate III. The sizes of the anticipated DNA fragments after *in vitro* digestion with *Eco*RI are presented below the figure.

In contrast, the corresponding native blot showed only two signals (bands e and f), with mobilities approximately corresponding to molecular sizes 1751 bp and 7421 bp, respectively (Fig. 3*B*).

To determine the nature of the DNA species designated c and d, the DNA samples restricted by *Eco*RI *in vitro* were further digested with S1 nuclease and examined by Southern blotting (Fig. 3*C*). DNA species designated c and d were both susceptible to S1 nuclease digestion, indicating that these DNAs contained single-stranded regions, and probably correspond to the DNA species designated e and f on the native blots.

The kinetics of ssDNA formation was assessed by densitometry of the autoradiogram from the native blot (i.e., DNA species e and f; Fig. 3*B*). The signal designated e increased and then decreased in intensity, in contrast to the signal designated f, which increased over the 105-min time course of the experiment (Fig. 3*D*).

These data indicated that resection from the *Xho*I cut site produced a ssDNA intermediate, and that resection proceeded past the proximal *Eco*RI site over time (manifest by the shift upward in molecular size of band e to band f; Fig. 3*B*).

Strand polarity was assigned to the ssDNA intermediates by hybridization of native blots with strand-specific oligonucleotide probes (Fig. 4). The progress of *in vivo* cutting by *Xho*I was monitored by probing a denatured blot containing *Pst*I-cut DNA isolated at 0, 15, and 60 min. In the latter two samples, the DNA bound probes specific for each strand and for each side of the *Xho*I cut (Fig. 4 *A*, *C*, *E*, and *G*). Probing the same DNAs under native conditions revealed binding of only those probes that were specific for chains ending 3′ at the *Xho*I cut site (Fig. 4 *B*, *D*, *F*, and *H*). These data demonstrate that the DNA restricted *in vivo* is subject, on both sides of the cut, to resection of the 5′-ended chains.

The above results were generalized by mutating λ's single *Xho*I cut site (through the insertion of an *Eco*RI linker at position 33498) and introducing a novel *Xho*I cut site into λ's

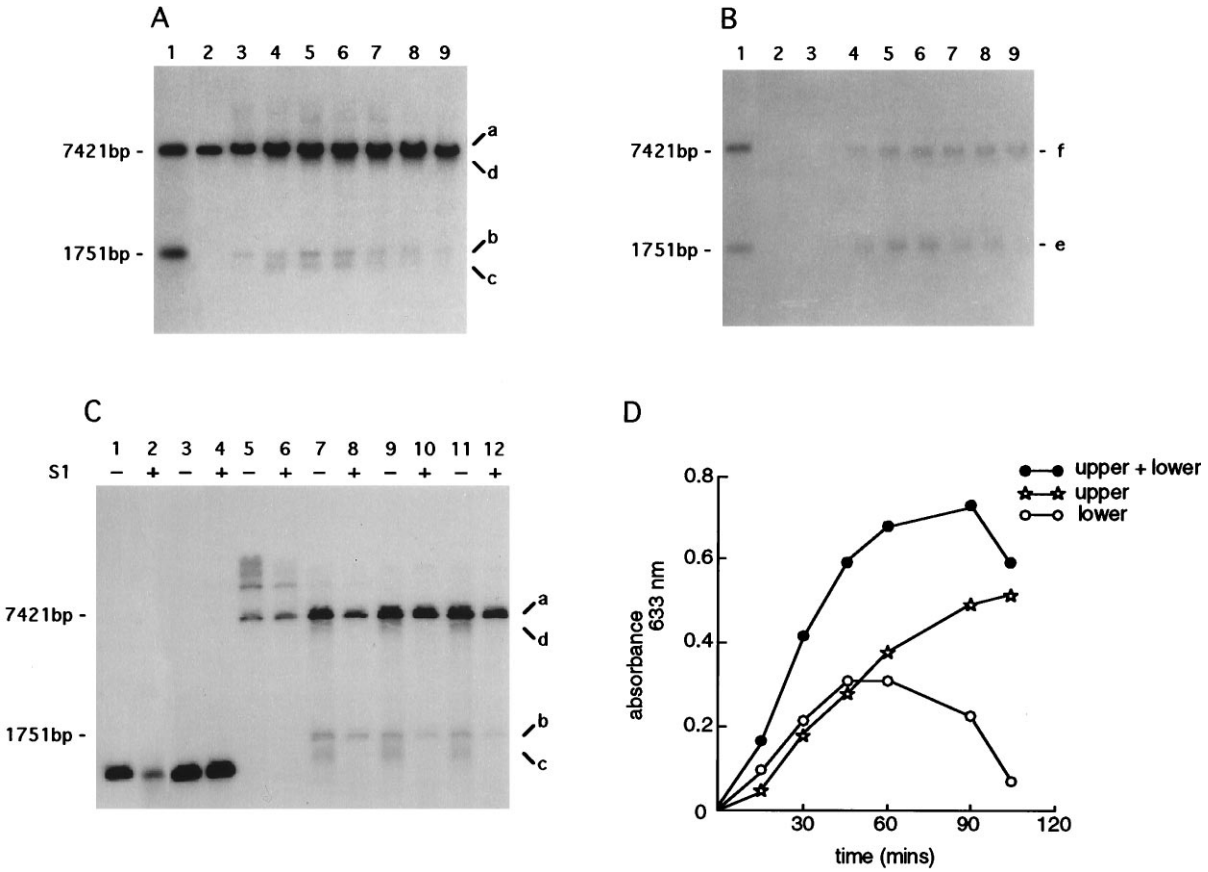

FIG. 3. Time course of the formation of ssDNA intermediates. An infection was established by wild-type λ (STU4) in strain FA77 (*rec*$^+$) carrying pPAORM3.8. Cells were harvested at 15-min intervals; total DNA extracts were prepared and digested *in vitro* with *Eco*RI. Gels were blotted onto nitrocellulose membranes under either Southern conditions (i.e., with denaturation) or native conditions (i.e., without denaturation). (*A*) Southern blot analysis of total DNA extracts digested *in vitro*. (*B*) Native blot of the same DNA samples as used in *A*. Lane 1, size standards for *Eco*RI digestion (7421 bp) and *Eco*RI/*Xho*I double digestion (1751 bp) of total λ DNA (see restriction map, Fig. 2); lanes 2–9, samples harvested at 15-min intervals; lane 2, time 0; lane 3, 15 min; lane 4, 30 min; lane 5, 45 min; lane 6, 60 min; lane 7, 75 min; lane 8, 90 min; and lane 9, 105 min. Each blot was probed with oligonucleotide 54 (position indicated in Fig. 2) designed to hybridize with single-strand overhangs of 3′ polarity. Signals designated a, b, c, d, e, and f indicate DNA intermediates referred to in the text. (*C*) Southern analysis of DNAs treated with S1 nuclease. DNA samples were either untreated (−) or treated (+) with 1 unit of S1 nuclease, except for lane 2, which was treated with 10 units. Lanes 1, 2, 3, and 4, represent a gel-purified *Xho*I/*Pst*I λ fragment and serve as the control for nuclease digestion; lanes 5–12, samples harvested at 15-min intervals and digested *in vitro* with *Eco*RI; lanes 5 and 6, time 0; lanes 7 and 8, 15 min; lanes 9 and 10, 30 min; and lanes 11 and 12, 60 min. The blot was probed with oligonucleotide 54. Signals designated a, b, c, and d correspond to those in *A*. (*D*) Densitometric scanning of the native blot presented in *B*. "Lower" refers to the signal at 1751 bp; "upper" refers to the signal at 7421 bp; "upper + lower" indicates the sum of the two signals.

leftmost *Eco*RI site (through insertion of an *Xho*I linker at position 21226; Tables 1 and 2; data not shown).

Involvement of λ's Red Functions in the Formation of ssDNA Intermediates. Table 3 summarizes ssDNA formation after infections with various Red mutants. In the absence of the Redα polypeptide (*b1451* and *red329* crosses), in both *rec*$^+$ and *recJ* hosts, ssDNA species of 3′ polarity were detected. ssDNA signals were absent when crosses were performed with phage that were doubly mutant for *red*α and λ's *ninR* region (*b1451 nin5* cross). To establish whether the Red gene products were sufficient to produce ssDNA recombination intermediates of 3′ polarity, crosses were performed with phage that carried simply a *nin5* deletion; in these crosses ssDNAs of 3′ polarity were observed. As identical observations were obtained in either *E. coli* wild-type or *recJ* backgrounds, the results demonstrate that the 3′ overhangs were not created by a helicase-assisted RecJ nuclease (32).

ssDNA intermediates could not be demonstrated in the following infections of a *rec*$^+$ host: (*i*) in the absence of the Redγ polypeptide (*gam210*; *gam210 nin5* crosses; Table 3); and (*ii*) in the simultaneous absence of both the Redα and Redβ polypeptides (*red15* cross; Table 3). However, somewhat surprisingly, ssDNA intermediates were observed under *rec*$^+$ and *recA* conditions with phage carrying a *sus* mutation in the *red*β gene (*red113* mutation).

Table 3. Effect of Red mutations on ssDNA formation

λ genotype	Red mutation	ssDNA rec$^{+*\dagger}$	ssDNA *recA**
Wild type		+	+
gam210	γ	−	−
gam210 nin5	γ	−	−
b1451	α	+	−
red329	α	+	ND
b1451 nin5	α	−	−
red113	β	+	+
red113 nin5	β	+	+
red15	α/β	−	ND
nin5		+	+

ND, not determined.
*Presence or absence of signal on native blots. For all genotypes, the corresponding denatured blot showed a strong signal corresponding to the *Xho*I double strand cut fragment.
†Identical observations in *E. coli rec*$^+$ and *recJ* hosts.

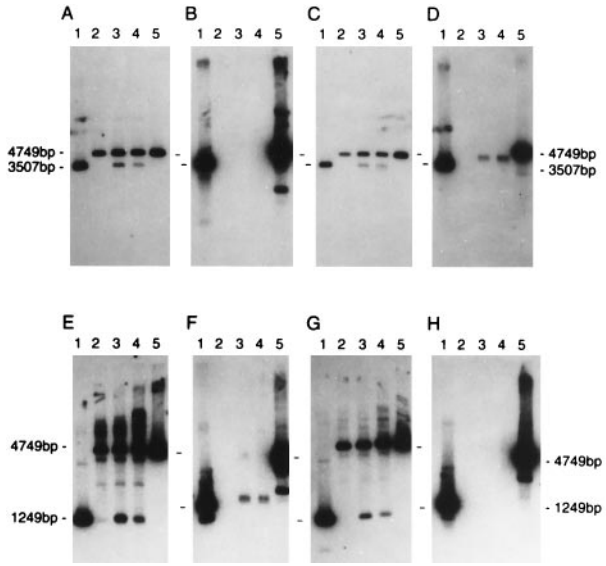

FIG. 4. Strand specificity of ssDNA intermediates. Wild-type λ (STU4)-infected strain FWS2520 (*recJ*) carrying pPAORM 3.8. Cells were harvested at time 0, 15 min, and 60 min into the infection. The series of blots presented in *A–H* are of total DNA extracts digested *in vitro* with *Pst*I (expected DNA fragment sizes following *in vitro Pst*I digestion: uncut modified phage DNA, 4749 bp; *Xho*I–*Pst*I fragment to the right of the *Xho*I cut site, 3507 bp; and *Xho*I–*Pst*I fragment to the left of the *Xho*I cut site, 1249 bp). Gels *A–D* examine events to the right of the *Xho*I cut site; gels *E–H* examine events to the left. *A*, *C*, *E*, and *G* are denatured blots; *B*, *D*, *F*, and *H* are native blots. *A* and *B* are hybridized with probe 250 (5′ specificity); *C* and *D*, with probe 249 (3′ specificity); *E* and *F*, with probe 54 (3′ specificity); and *G* and *H*, with probe 53 (5′ specificity). Lanes 1 and 5 in each gel are the size standards *Pst*I/*Xho*I (3507 bp and 1249 bp) and *Pst*I (4749 bp) (denatured native blot size standards were obtained by boiling the restricted DNAs immediately prior to electrophoresis); experimental samples are in lane 2 (time 0), lane 3 (15 min), and lane 4 (60 min).

Kinetic Analysis of ssDNA Formation. The preceding data indicate that both the Redα exonuclease and a *ninR*-encoded function(s) are likely contributors to the ssDNA intermediates demonstrated in Fig. 3*B*. To elucidate the separate contributions of Red and NinR on the formation of ssDNA intermediates, a kinetic analysis was undertaken on infections (wild-type, *b1451*, *nin5*, and *b1451 nin5* phage) performed simultaneously on the same batch of cells (Fig. 5). A comparison of the native hybridization patterns (Fig. 5 *B* and *C*) allows the following conclusions: (*i*) ssDNA intermediates that are detectable at early time points (15 min) arise primarily through the action of Redα exonuclease (*nin5* cross); (*ii*) ssDNA that is detected at later time points (90 min) results primarily from the action of the *ninR* function (*b1451* cross; (*iii*) Redα exonuclease contributes more to resection from DSBs than its *ninR* counterpart; and (*iv*) the pattern of ssDNA formation generated with wild-type phage is a composite consisting of ssDNA generated by the Redα exonuclease and the *ninR* function.

DISCUSSION

Genetic and biochemical analyses of λ's Red recombination pathway had predicted ssDNA intermediates of 3′ polarity (1, 3, 5, 6). The physical analyses performed in this *in vivo* study accord with these predictions. Furthermore, the ssDNA intermediates are long-lived (possibly >105 min), may exceed 1.4 kb in length, and are produced bidirectionally from a DSB, in the two intervals examined.

The expected dependence of ssDNA formation on Redα was demonstrable only in a *nin5* background. The *ninR* region may contribute an exonuclease with properties similar to those of Redα. Alternatively, the *ninR* region may contribute an inhibitor of an unspecified nuclease that is active on 3′-ended ssDNA. Phage carrying the *nin5* deletion enjoy wild-type levels of recombination, implying that NinR-dependent ssDNAs do not participate in any major way in the formation of recombinants in Red^+ $RecA^+$ infections when DNA replication is blocked (T. Tarkowski, personal communication). The data in Fig. 5 show that the *red*α- and *ninR*

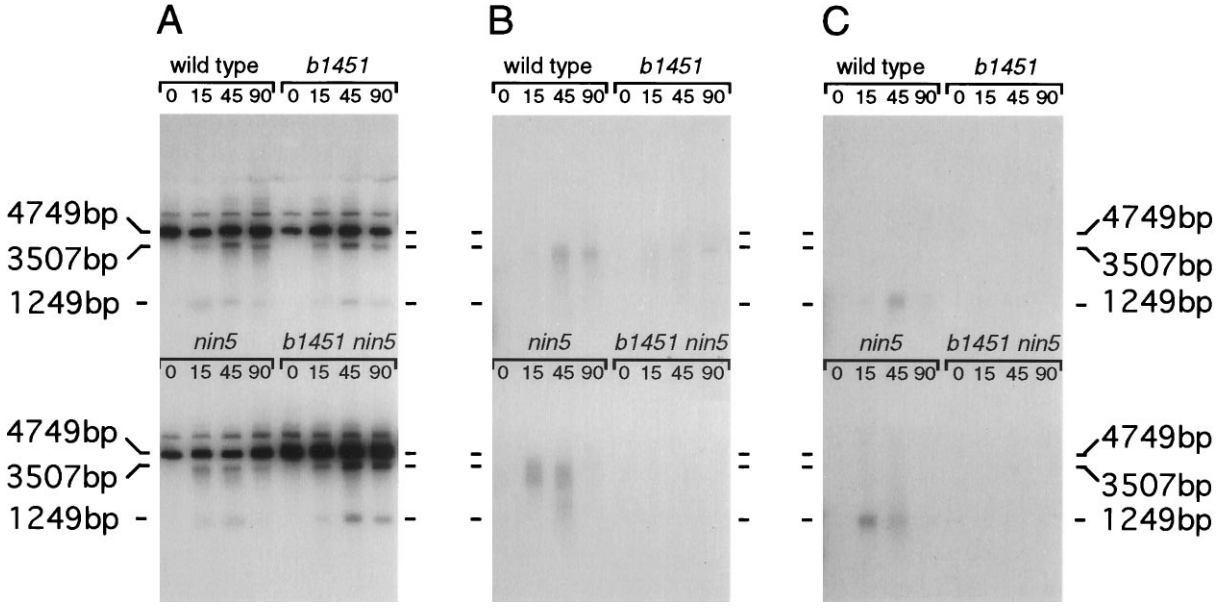

FIG. 5. Kinetic analysis of ssDNA formation. Concurrent rec^+ infections were established with λ: wild type, *b1451*, *nin5*, and *b1451 nin5*. Total DNA extracts were prepared from cells recovered at times 0, 15 min, 45 min, and 90 min. Each sample was digested *in vitro* with *Pst*I prior to electrophoresis and blotting. (*A*) Denatured blot probed with two random-primed DNA fragments that recognize λ DNA to the right and to the left of the *Xho*I cut site. (*B*) Native blot probed with a random-primed DNA fragment that recognizes λ DNA to the right of the *Xho*I cut site. (*C*) Native blot probed with a random-primed DNA fragment that recognizes λ DNA to the left of the *Xho*I cut site. Size markers align with λ DNA cleaved with *Pst*I (4749 bp) and *Pst*I/*Xho*I (3507 bp and 1249 bp).

exonucleolytic effects are temporally separated. Early (Redα-generated) ssDNA intermediates rise and fall in intensity as the infection proceeds; late (NinR-generated) ssDNA intermediates accumulate over time (cf. *b1451* and *nin5* crosses, Fig. 5 *B* and *C*). These kinetic distinctions suggest that the loss of signal from the Redα-generated ssDNA species was due to the incorporation of these early ssDNA intermediates into intermediates further advanced along the Red pathway, whereas the NinR-generated ssDNAs are unsuitable for recombination. The appearance and disappearance of ssDNAs are also seen in *S. cerevisiae* after induction of the mating-type switch (33). In λ crosses, using Red functions supplied by a plasmid (34), recombinant molecules are observed as early as 20 min after infection and accumulate for up to 2 hr subsequent to synchronous *in vivo* restriction cutting (A. Kuzminov, personal communication). These kinetics suggest that the ssDNAs shown in this study do represent the predicted first intermediate in the Red pathway.

The longevity of the ssDNA intermediates invites comment. To survive for so long (possibly >105 min), these ssDNA intermediates must be protected from nucleases. Cassuto and Radding (35) proposed that the formation of single-strand intermediates involving the Redα/β polypeptides is a coupled reaction (35). In their view, Redα exonuclease operates in concert with the Redβ polypeptide, with β protein either coating and protecting the nascent strand as it is being formed or facilitating incorporation of the nascent strand into the homologous duplex. Our data only partially support the Cassuto and Radding model. We found reduced amounts of ssDNA in the absence of Redβ (either with or without the *ninR*-encoded functions). However, ssDNA intermediates were observed in the absence of Redβ (in both *rec*$^+$ and *recA* backgrounds), indicating that the presence of neither Redβ nor RecA is essential for Redα exonuclease to operate.

Several mechanistic parallels have been established between the λ Red pathway and the alternative RecE recombination pathway in *E. coli* (reviewed in ref. 36). RecE recombination is observed in *E. coli recB recC sbcA* mutants, where suppressor-mediated derepression of the Rac prophage activates a 5′-3′-exonuclease (the *recE* gene product) and an annealing protein (the *recT* gene product) with biochemical properties similar to those of the Redα/β proteins (36). *sbcA* mutations are able to complement both *red*α and *red*β mutations (37, 38), and genetic analysis has shown that the RecE and RecT polypeptides can operate on DSBs when delivered to defined plasmid DNAs (39), yielding heteroduplexes with predicted 3′ strand polarities (40). However, the RecE/RecT polypeptides appear less efficient at operating at DSBs than the Redα/β proteins (39), which may indicate a difference in how the two sets of proteins recognize a DSB. The *in vivo* assays employed in this study should be able to establish whether long stable ssDNAs are also found in the RecE pathway.

The longevity of the Red intermediates and the tractability of the λ/*E. coli* system encourages further investigation of the "*in vivo* biochemistry" of Red-mediated DSB-induced recombination.

We thank members of the Stahl laboratory for helpful comments on this manuscript. Trudee Tarkowski's suggestions played a major role in the shaping of this work. S.A.H. thanks Jim Sawitzke and Kit Tilly for help with λ biology. Susan Smaus, Gary Hettrick, and Bob Evans helped in the preparation of this manuscript for publication. This work was supported by National Institutes of Health Grant GM-33677 and National Science Foundation Grant MCB-9402695. F.W.S. is American Cancer Society Research Professor of Molecular Biology.

1. Stahl, F. W., Kobayashi, I. & Stahl, M. M. (1985) *J. Mol. Biol.* **181,** 199–209.
2. Stahl, F. W., Fox, M. S., Faulds, D. & Stahl, M. M. (1990) *Genetics* **125,** 463–474.
3. White, R. L. & Fox, M. S. (1974) *Proc. Natl. Acad. Sci. USA* **71,** 1544–1548.
4. Stahl, F. W., McMilin, K. D., Stahl, M. M., Crasemann, J. M. & Lam, S. (1974) *Genetics* **77,** 395–408.
5. Siddiqi, I., Stahl, M. M. & Stahl, F. W. (1991) *Genetics* **128,** 7–22.
6. Little, J. W. (1967) *J. Biol. Chem.* **242,** 679–686.
7. Carter, D. M. & Radding, C. M. (1971) *J. Biol. Chem.* **246,** 2502–2512.
8. Sriprakash, K. S., Lund, N., Huh, M. M. & Radding, C. M. (1975) *J. Biol. Chem.* **250,** 5438–5445.
9. Thaler, D. S., Stahl, M. M. & Stahl, F. W. (1987) *J. Mol. Biol.* **195,** 75–87.
10. Connolly, B., White, C. I. & Haber, J. E. (1988) *Mol. Cell. Biol.* **8,** 2342–2349.
11. White, C. I. & Haber, J. E. (1990) *EMBO J.* **9,** 663–673.
12. Kolodkin, A. L., Klar, A. J. S. & Stahl, F. W. (1986) *Cell* **46,** 733–740.
13. Nicolas, A., Treco, D., Schultes, N. P. & Szostak, J. W. (1989) *Nature (London)* **338,** 35–38.
14. Sun, H., Treco, D., Schultes, N. P. & Szostak, J. W. (1989) *Nature (London)* **338,** 87–90.
15. Szostak, J. W., Orr-Weaver, T. L., Rothstein, R. J. & Stahl, F. W. (1983) *Cell* **33,** 25–35.
16. Sun, H., Treco, D. & Szostak, J. W. (1991) *Cell* **64,** 1155–1161.
17. Rudin, N., Sugarman, E. & Haber, J. E. (1989) *Genetics* **122,** 519–534.
18. McMilin, K. D. & Russo, V. E. A. (1972) *J. Mol. Biol.* **68,** 49–55.
19. Gingeras, T. R. & Brooks, J. E. (1983) *Proc. Natl. Acad. Sci. USA* **80,** 402–406.
20. Sussman, R. & Jacob, F. (1962) *C. R. Acad. Sci.* **254,** 1517–1519.
21. Campbell, A. (1961) *Virology* **14,** 22–32.
22. Goldberg, A. R. & Howe, M. (1969) *Virology* **38,** 200–202.
23. Daniels, D. L., Schroeder, J. L., Szybalski, W., Sanger, F. & Blattner, F. R. (1983) in *Lambda II*, eds. Hendrix, R. W., Roberts, J. W., Stahl, F. W. & Weisberg, R. A. (Cold Spring Harbor Lab. Press, Plainview, NY), pp. 469–676.
24. Shulman, M. J., Hallick, L. M., Echols, H. & Signer, E. R. (1970) *J. Mol. Biol.* **52,** 501–520.
25. Zissler, J., Signer, E. & Schaefer, F. (1971) in *The Bacteriophage Lambda*, ed. Hersey, A. D. (Cold Spring Harbor Lab. Press, Plainview, NY), pp. 455–469.
26. Court, D. & Sato, K. (1969) *Virology* **39,** 348–352.
27. Arber, W., Enquist, L., Hohn, B., Murray, N. E. & Murray, K. (1983) in *Lambda II*, eds. Hendrix, R. W., Roberts, J. W., Stahl, F. W. & Weisberg, R. A. (Cold Spring Harbor Lab. Press, Plainview, NY), pp. 433–466.
28. Ausubel, F. M., Brent, R., Kingston, R. E., Moore, D. D., Seidman, J. G., Smith, J. A. & Struhl, K. (1989) *Current Protocols in Molecular Biology 1* (Greene & Wiley, New York).
29. Lichten, M. J. & Fox, M. S. (1983) *Nucleic Acids Res.* **11,** 3959–3971.
30. Southern, E. (1975) *J. Mol. Biol.* **98,** 503–513.
31. Better, M. & Freifelder, D. (1983) *Virology* **126,** 168–182.
32. Kowalczykowski, S. C., Dixon, D. A., Eggleston, A. K., Lauder, S. D. & Rehrauer, W. M. (1994) *Microbiol. Rev.* **58,** 401–465.
33. Sugawara, N. & Haber, J. E. (1992) *Mol. Cell Biol.* **12,** 563–575.
34. Poteete, A. R. & Fenton, A. C. (1993) *Genetics* **134,** 1013–1021.
35. Cassuto, E. & Radding, C. M. (1971) *Nature (London) New Biol.* **229,** 13–16.
36. Kolodner, R., Hall, S. D. & Luisi-Luca, C. (1994) *Mol. Microbiol.* **11,** 23–30.
37. Gillen, J. R. & Clark, A. J. (1974) in *Mechanism of Recombination*, ed. Grell, R. F. (Plenum, New York), pp. 123–136.
38. Gillen, J. R., Willis, D. K. & Clark, A. J. (1981) *J. Bacteriol.* **145,** 521–532.
39. Yokochi, T., Kusano, K. & Kobayashi, I. (1995) *Genetics* **139,** 5–17.
40. Silberstein, Z., Tzfati, Y. & Cohen, A. (1995) *J. Bacteriol.* **177,** 1692–1698.